Acta Crystallographica Section F
Structural Biology Communications
ISSN 2053-230X

Expression, purification and X-ray crystallographic analysis of the *Helicobacter pylori* blood group antigen-binding adhesin BabA

Suresh Subedi,[a,b] Kristof Moonens,[a,b] Ema Romão,[c,d] Alvin Lo,[a,b] Guy Vandenbussche,[e] Jeanna Bugaytsova,[f] Serge Muyldermans,[c,d] Thomas Borén[f] and Han Remaut[a]*

[a]Structural and Molecular Microbiology, VIB Department of Structural Biology, VIB, Pleinlaan 2, 1050 Brussels, Belgium, [b]Structural Biology Brussels, Vrije Universiteit Brussel, Pleinlaan 2, 1050 Brussels, Belgium, [c]Research Group Cellular and Molecular Immunology, Vrije Universiteit Brussel, Pleinlaan 2, 1050 Brussels, Belgium, [d]Structural Biology Research Center, VIB, Vrije Universiteit Brussels, Pleinlaan 2, 1050 Brussels, Belgium, [e]Structure and Function of Biological Membranes, Université Libre de Bruxelles, Boulevard du Triomphe, 1050 Brussels, Belgium, and [f]Department of Medical Biochemistry and Biophysics, Umeå University, SE-901 87 Umeå, Sweden

Correspondence e-mail: han.remaut@vib-vub.be

Received 17 September 2014
Accepted 21 October 2014

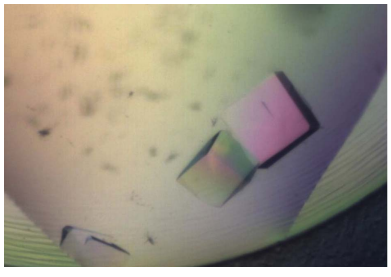

Helicobacter pylori is a human pathogen that colonizes about 50% of the world's population, causing chronic gastritis, duodenal ulcers and even gastric cancer. A steady emergence of multiple antibiotic resistant strains poses an important public health threat and there is an urgent requirement for alternative therapeutics. The blood group antigen-binding adhesin BabA mediates the intimate attachment to the host mucosa and forms a major candidate for novel vaccine and drug development. Here, the recombinant expression and crystallization of a soluble BabA truncation ($BabA^{25–460}$) corresponding to the predicted extracellular adhesin domain of the protein are reported. X-ray diffraction data for nanobody-stabilized $BabA^{25–460}$ were collected to 2.25 Å resolution from a crystal that belonged to space group $P2_1$, with unit-cell parameters $a = 50.96$, $b = 131.41$, $c = 123.40$ Å, $\alpha = 90.0$, $\beta = 94.8$, $\gamma = 90.0^\circ$, and which was predicted to contain two $BabA^{25–460}$–nanobody complexes per asymmetric unit.

1. Introduction

Helicobacter pylori is a Gram-negative bacterium that colonizes the gastric mucosa of about 50% of the world's population. Unless treated with antibiotics, *H. pylori* infections are usually persistent and are associated with chronic gastric inflammation, which in symptomatic carriers can develop into gastric and duodenal ulcers and even gastric malignancies such as mucosa-associated lymphoid tissue (MALT) lymphoma and gastric adenocarcinoma (Every, 2013).

H. pylori infection is dependent on a complex interplay between the bacterium and its human host. Apart from environmental factors and host genetic predisposition, a number of *H. pylori* virulence factors are associated with more severe clinical outcomes of infection (Delahay & Rugge, 2012; Backert & Clyne, 2011). Along with the secreted virulence factors CagA and VacA, another important virulence trait of *H. pylori* is the ability to strongly adhere to the gastric mucosa. The blood group antigen-binding adhesin (BabA) is a major adhesin that interacts with fucosylated Lewis b (Le^b) and H type 1 blood group antigens on the surface of human gastric epithelial cells (Borén *et al.*, 1993; Aspholm-Hurtig *et al.*, 2004; Moore *et al.*, 2011). The reference strain CCUG17875 possesses two *babA* genes: a silent *babA1* locus and a *babA2* gene that is expressed as functional BabA adhesin (Ilver *et al.*, 1998). In conjunction with the *cagA* and *vacA* s1 alleles, a *babA2*-positive genotype is found to be associated with duodenal ulcer disease and gastric cancer (Gerhard *et al.*, 1999).

In recent years, multidrug-resistant *H. pylori* strains have spread worldwide, creating a demand for new therapeutics that can both treat and prevent infections. In Gram-negative bacteria, secretion pathways play an important role in pathogenesis and recent studies have focused on chemotherapeutics for the directed intervention in secretion machineries such as bacterial pili that mediate host-cell adhesion (Lo *et al.*, 2013).

Hence, in a quest for the rational design of structure-based anti-adhesives, we initiated structural characterization of the BabA–Le^b interaction. BabA is one of the members of the *Helicobacter* outer membrane porin (HOP) family. Comparative genome analysis and predicted secondary-structure analysis of HOP adhesins highlight a conserved C-terminal domain predicted to be the corresponding

Table 1
Cloning of BabA truncations.

Source organism	*H. pylori*
DNA source	*H. pylori* CCUG 17875 *babA2* gene (accession No. AF033654.1)
Forward primer: BabA_IbaHR4-f	5′-ATGGTAGGTCTCAGGCCGAAGACGACGGCTTTTACACAAGCG-3′
Reverse primer: BabA_IbaHR4_460-r	5′-GTCGTAGGTCTCAGCGCTGAAATTCACTAGAGTGTCAGCGATGTTTTC-3′
Reverse primer: BabA_IbaHR4_480-r	5′-GTCGTAGGTCTCAGCGCTTTTGGAGAGCGCAGTAGTGATGCTG-3′
Reverse primer: BabA_IbaHR4_523-r	5′-GTCGTAGGTCTCAGCGCTTGATATCTAACTAAGCTTGACCTGTGAAGTG-3′
Reverse primer: BabA_IbaHR4_546-r	5′-GTCGTAGGTCTCAGCGCTCCCATTCATGGCACCATTGTTGGTTTGAGAAC-3′
Forward primer: BabA_IbaHR3-f	5′-ATGGTAGGTCTCACTCCGGCATCCAAGATCTTTCAGACAACTATG-3′
Reverse primer: BabA_IbaHR3-r	5′-GTCGTAGGTCTCATATCAGTGATGGTGATGGTGATGCGATCCTC-3′
Cloning vectors	pASK-HR3, pASK-HR4

Table 2
Crystallization of BabA$^{25–460}$–Nb-ER19.

Method	Sitting-drop vapour diffusion
Plate type	MRC 96-well crystallization plate (Swissci)
Temperature (K)	293
Protein concentration (mg ml^{-1})	15
Buffer composition of protein solution	20 m*M* sodium acetate pH 5.0, 150 m*M* NaCl, 5% glycerol
Composition of reservoir solution	0.2 *M* sodium nitrate; 0.1 *M* bis-tris propane pH 6.5, 20%(*w*/*v*) PEG 3350
Volume and ratio of drop	0.4 µl, 1:1
Volume of reservoir (µl)	50

membrane-anchoring β-barrel domain, which is preceded by a variable domain that is expected to contain the adhesive properties (Tomb *et al.*, 1997; Alm *et al.*, 2000). This architecture is reminiscent of autotransporter-like proteins, in which a C-terminal β-barrel guides the secretion of an N-terminally located passenger domain. Here, we report the expression and purification of a BabA truncation corresponding to the putative N-terminal adhesin domain and show that an N-terminal construct spanning amino-acid residues 25–460 can be expressed as a stable folded unit. We further report on the crystallization of the N-terminal soluble adhesin domain with the aid of nanobodies, which are camelid-derived single-domain antibodies that have successfully been used as crystallization chaperones, for example in the case of conformationally complex or aggregating proteins (Steyaert & Kobilka, 2011; Baranova *et al.*, 2013).

2. Materials and methods

2.1. Cloning, expression and purification of BabA truncations

DNA coding sequences corresponding to the BabA fragments BabA$^{1–460}$, BabA$^{1–480}$, BabA$^{1–496}$, BabA$^{1–523}$ and BabA$^{1–546}$ were PCR-amplified from *H. pylori* CCUG 17875 genomic DNA using primers (the forward primer BabA_IbaHR4-f and the reverse primers BabA_IbaHR4_460-r, BabA_IbaHR4_480-r, BabA_IbaHR4_523-r and BabA_IbaHR4_546-r) shown in Table 1. The amplicons were digested with *Bsa*I and cloned into pASK-HR4, a derivative of the pASK-IBA32 vector (IBA GmbH) with the N-terminal *ompA* leader sequence replaced by the *dsbA* leader. DNA fragments corresponding to BabA$^{25–460}$, BabA$^{25–480}$, BabA$^{25–523}$ and BabA$^{25–546}$ were PCR-amplified from their respective pASK-HR4 parent constructs using primers (forward primer BabA_IbaHR3-f and reverse primer BabA_IbaHR3-r) as provided in Table 1, digested with *Bsa*I and cloned into pASK-HR3, a pASK-IBA12-derived vector in which the *ompA* leader sequence was replaced by the *dsbA* leader. Thus, the resulting BabA fragments comprise an N-terminal DsbA signal peptide for periplasmic expression followed by a thrombin-cleavable Strep-tag II and a 6×His tag at their C-terminal end. *Escherichia coli* TOP10 cells were transformed with the pASK-HR3 or pASK-HR4 constructs, grown on lysogeny broth (LB) supplemented with 100 mg ml^{-1} ampicillin until an OD_{600} of 0.7 was reached and induced overnight at 293 K with 0.2 mg ml^{-1} anhydrotetracycline.

For large-scale expression for functional and structural analysis, TOP10 cells grown and induced as described above were harvested by centrifugation at 6238*g* for 15 min at 277 K using a JA-8.1 rotor in an Avanti-J26 XP Beckman Centrifuge. Periplasmic extraction was performed by suspending the cells in 4 ml 20 m*M* Tris–HCl pH 8.8, 20%(*w*/*v*) sucrose (per 1 g of wet cell pellet) with the protease inhibitors AEBSF–HCl (0.4 m*M*) and leupeptin (1 mg ml^{-1}) followed by treatment with 40 µl 0.5 *M* EDTA and 40 µl lysozyme (10 mg ml^{-1}) and mixing gently on ice for 20 min. 80 µl 1 *M* $MgCl_2$ was added and the periplasmic extract was cleared from spheroplasts by centrifugation at 17 418*g* for 20 min at 277 K in a JA-20 rotor. The periplasmic extract was further clarified by centrifugation at 48 384*g* for 30 min at 277 K in the same rotor and filtered through a 0.45 µm syringe filter.

BabA fragments were purified by consecutive nickel and Strep-Tactin affinity chromatography. Briefly, the periplasmic extract was loaded onto a 5 ml pre-packed Ni–NTA column (GE Healthcare) pre-equilibrated with buffer *A* (20 m*M* Tris–HCl pH 8.8, 250 m*M* NaCl, 5% glycerol), washed with five bed volumes of buffer *A* and the bound protein was eluted with 280 m*M* imidazole in buffer *A*. Eluted peak fractions were collected and loaded onto a 5 ml pre-packed Strep-Tactin column (IBA GmbH) equilibrated with buffer *C* (20 m*M* Tris–HCl pH 8.8, 150 m*M* NaCl, 5% glycerol), washed with five bed volumes of buffer *C* and the bound protein was eluted with 0.6 mg ml^{-1} D-desthiobiotin in buffer *C*. In addition to the crystallization trials for these BabA truncations, we opted for a nanobody-aided crystallization approach. For this purpose, we used Nb-ER19, a nanobody raised against native full-length BabA purified from the outer membrane of *H. pylori* strain CCUG 17875. Nb-ER19 was produced and purified as described elsewhere (Baranova *et al.*, 2013; Pardon *et al.*, 2014).

To form BabA–Nb-ER19 complexes, the periplasmic extracts of the BabA truncations (BabA$^{25–460}$, BabA$^{25–523}$ and BabA$^{25–546}$) and Nb-ER19 were mixed in a 5:1(*v*:*v*) ratio on ice and nickel-affinity purification was performed as described above. Fractions containing the respective BabA fragments and Nb-ER19 were pooled and concentrated in a 10 kDa molecular-weight cutoff spin concentrator to a final volume of 500 µl. The concentrated sample was then loaded onto a Superdex S-200 16/60 column (GE Healthcare) pre-equilibrated with 20 m*M* sodium acetate pH 5.0, 150 m*M* NaCl, 5% glycerol. Eluted fractions containing the BabA–Nb-ER19 complex, with the affinity purification tags intact, were pooled and concentrated to a final concentration of 15 mg ml^{-1} using a 10 kDa molecular-weight cutoff spin concentrator prior to crystallization.

2.2. Crystallization

Crystallization of BabA$^{1–460}$, BabA$^{25–460}$ and its complex with Nb-ER19 was first screened at 293 K by the sitting-drop vapour-diffusion method with commercial sparse-matrix crystallization screening kits [SaltRx, SaltRx 2, Grid Screen Salt HT, PEGRx 2, Index HT (Hampton Research), JBScreen Basic, JBScreen Classic, JBScreen PEG/Salt (Jena Bioscience) and PACT *premier* HT-96, JCSG-*plus* HT-96 and ProPlex HT-96 (Molecular Dimensions)] in 96-well MRC plates. Each crystallization drop was prepared by mixing 400 nl

Table 3
Data collection and processing.

Values in parentheses are for the outer shell.

Diffraction source	I04, Diamond Light Source
Wavelength (Å)	0.97949
Temperature (K)	100
Detector	PILATUS 6M CCD
Crystal-to-detector distance (mm)	385.01
Rotation range per image (°)	0.2
Total rotation range (°)	200
Exposure time per image (s)	0.2
Space group	$P12_11$
a, b, c (Å)	50.96, 131.41, 123.40
α, β, γ (°)	90.0, 94.8, 90.0
Mosaicity (°)	0.16
Resolution range (Å)	65.71–2.25 (2.31–2.25)
Total No. of reflections	339889
No. of unique reflections	76055
Completeness (%)	99.2 (100.0)
Multiplicity	4.5 (4.5)
$\langle I/\sigma(I)\rangle$	14.5 (2.2)
R_{meas} (%)	6.3 (79.0)
Overall B factor from Wilson plot (Å^2)	43.6

protein solution and 400 nl reservoir solution (a 1:1 ratio) and equilibrating against 50 µl reservoir solution. Crystallization information is summarized in Table 2.

2.3. Data collection and processing

A BabA$^{25–460}$–Nb-ER19 crystal grown in 0.2 *M* sodium nitrate, 0.1 *M* bis-tris propane pH 6.5, 20%(*w*/*v*) PEG 3350 and supplemented with 10% glycerol was mounted in a SPINE-standard nylon loop and flash-cooled in liquid nitrogen. Diffraction data for the native protein were collected on beamline I04 at Diamond Light Source, Didcot, England equipped with a PILATUS 6M CCD detector. The diffraction data were processed with *XDS* and *xia*2 (Kabsch, 2010) and truncated to 2.25 Å resolution on the basis of an $I/\sigma(I)$ cutoff of 2. The crystals belonged to the monoclinic space group $P2_1$, with unit-cell parameters a = 50.960, b = 131.410, c = 123.40 Å, α = 90.00, β = 94.80, γ = 90.00°, compatible with two to three BabA$^{25–460}$–Nb-ER19 complexes per asymmetric unit, corresponding to a calculated V_M of 3.3 and 2.2 Å^3 Da^{-1} and a solvent content of 60 and 41%, respectively (Matthews, 1968). Crystallographic data statistics are presented in Table 3.

3. Results and discussion

On the basis of comparative genome analysis and secondary-structure prediction of HOP adhesins, we made C-terminal truncation constructs that remove the predicted β-barrel domain. In this way,

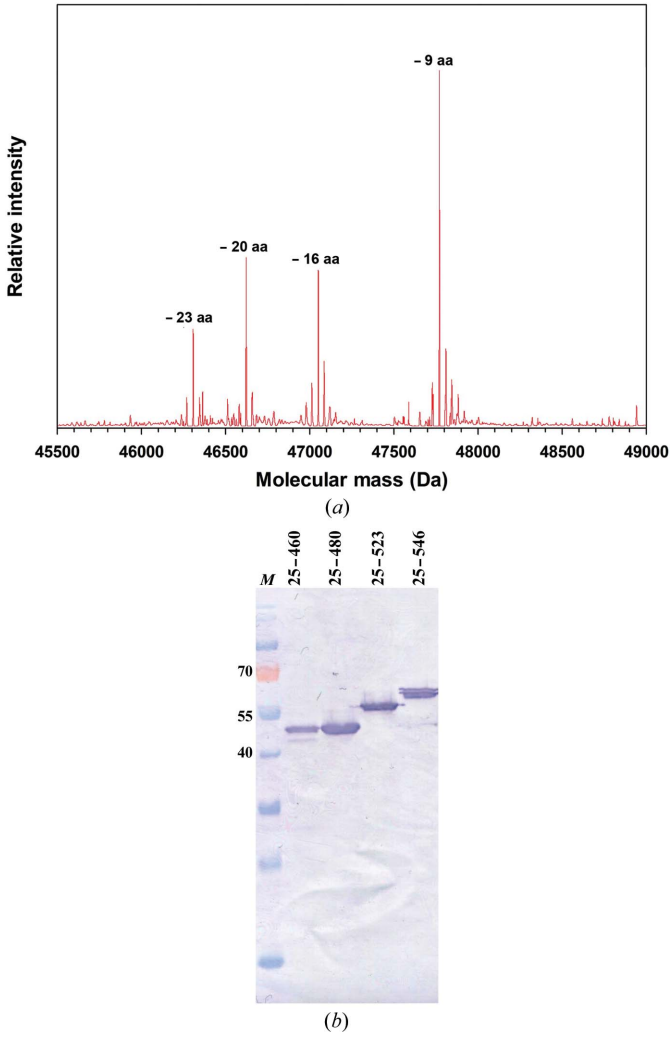

Figure 1
(*a*) MS spectra of BabA$^{1–460}$ reveal spontaneous proteolysis leading to the loss of up to 23 N-terminal amino acids. (*b*) Immunoblot detection (using α-His antibody) of BabA fragments in the respective periplasmic extracts. Lane *M* contains molecular-mass marker (labelled in kDa).

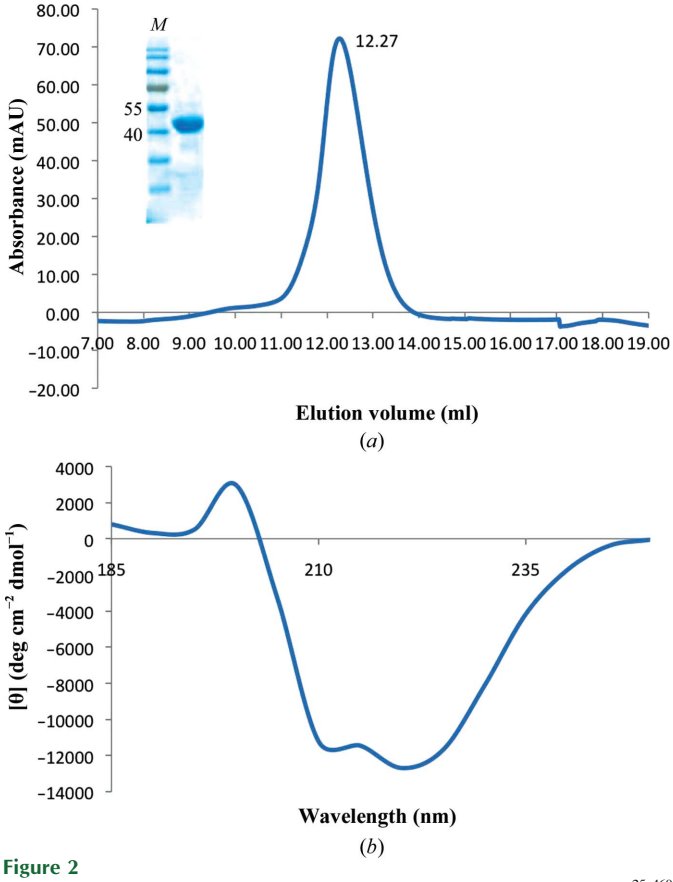

Figure 2
(*a*) Size-exclusion chromatogram and SDS–PAGE analysis (inset) of BabA$^{25–460}$ run on Superdex 75 10/300 (GE Healthcare). (*b*) CD spectrum of BabA$^{25–460}$ in phosphate buffer (50 m*M* KH_2PO_4/K_2HPO_4 pH 8.0) reveals a predominantly α-helical secondary-structure content.

five constructs were generated with truncation sites falling in-between predicted secondary-structure elements upstream of the C-terminal β-strand region: BabA$^{1–460}$, BabA$^{1–480}$, BabA$^{1–496}$, BabA$^{1–523}$ and BabA$^{1–546}$. Although these constructs were found to result in the expression of recombinant protein of the expected molecular weight, the expression products were mostly found in the insoluble fraction and the protein fractions purified from the periplasmic extracts were found to be prone to aggregation. Mass-spectrometric analysis showed the rapid proteolytic loss of the first 23 N-terminal residues (Fig. 1*a*), indicating these were not part of a stably folded core in the BabA truncates. Based on this susceptibility to degradation, we modified the *babA*$^{1–460}$, *babA*$^{1–480}$, *babA*$^{1–523}$ and *babA*$^{1–546}$ constructs to remove the first 24 amino acids of the mature protein. With the exception of BabA$^{25–480}$, the remaining N-terminal deletion constructs resulted in the periplasmic expression of soluble recombinant BabA fragments corresponding to the expected molecular weight (Fig. 1*b*).

On analytical size exclusion (Superdex 75 10/300; Fig. 2*a*), the minimal fragment, BabA$^{25–460}$, eluted as a single peak corresponding to a calculated molecular mass of about 52 kDa, matching that expected for a BabA$^{25–460}$ monomer with N-terminal and C-terminal tags (49 319 Da). When analysed by circular-dichroism (CD) spectroscopy, the BabA$^{25–460}$ truncation showed a folded conformation with a high α-helical secondary-structure content (Fig. 2*b*). A dominant α-helical secondary structure was also observed in the recently solved structure of the *H. pylori* HOP adhesin SabA (Pang *et al.*, 2014). Similar to BabA$^{25–460}$, expression of BabA$^{25–523}$ and BabA$^{25–546}$ resulted in folded recombinant BabA fragments (data not shown).

Recombinant proteins were concentrated to 10–15 mg ml^{-1} and subjected to crystallization trials using the commercially available sparse-matrix screens described above. Extensive screens for the BabA fragments did not result in the growth of single crystals in the conditions used. Hence, we opted for a nanobody-aided crystallization approach. Crystals of BabA$^{25–460}$–Nb-ER19 were obtained in multiple different conditions of the PACT *premier* and JCSG-*plus* screens after 1–2 d incubation at 293 K. Optimization of PACT *premier* screen condition F5 with differing PEG 4000 concentrations (16–24%) also led to the reproducible growth of cube-shaped crystals of average dimensions of 0.06 × 0.06 × 0.06 mm (Fig. 3*a*). SDS–PAGE analysis of washed and dissolved crystals confirmed that these contained both BabA$^{25–460}$ and Nb-ER19 (Fig. 3*a*, inset).

A crystal grown in 0.2 *M* sodium nitrate, 0.1 *M* bis-tris propane pH 6.5, 20%(*w*/*v*) PEG 3350 diffracted to at least 2.25 Å resolution (Fig. 3*b*). The crystal belonged to the monoclinic space group $P2_1$, with unit-cell parameters compatible with a predicted two or three BabA$^{25–460}$–Nb-ER19 complexes per asymmetric unit. Selenomethionine-derivatized protein is in production to allow experimental phase determination by a single anomalous dispersion experiment. The high-resolution structure of the BabA extracellular domain will be invaluable in understanding its ligand-binding properties and is anticipated to facilitate the development of anti-adhesive compounds that may serve as novel therapeutic and/or prophylactic eradication therapies against *H. pylori*.

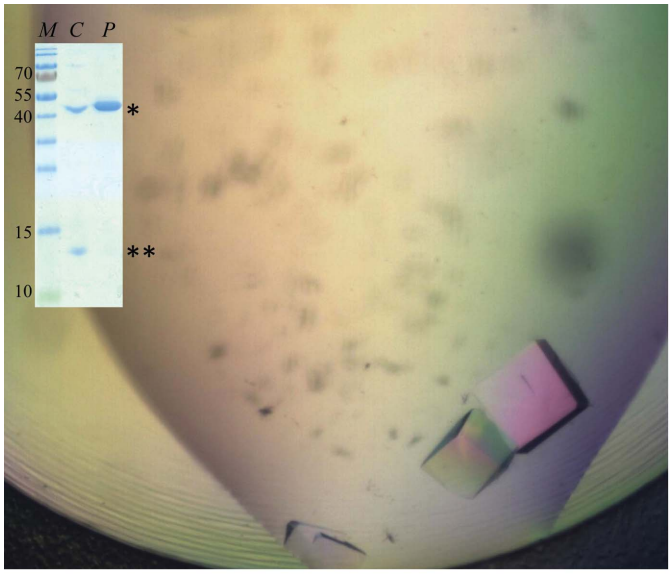

(*a*)

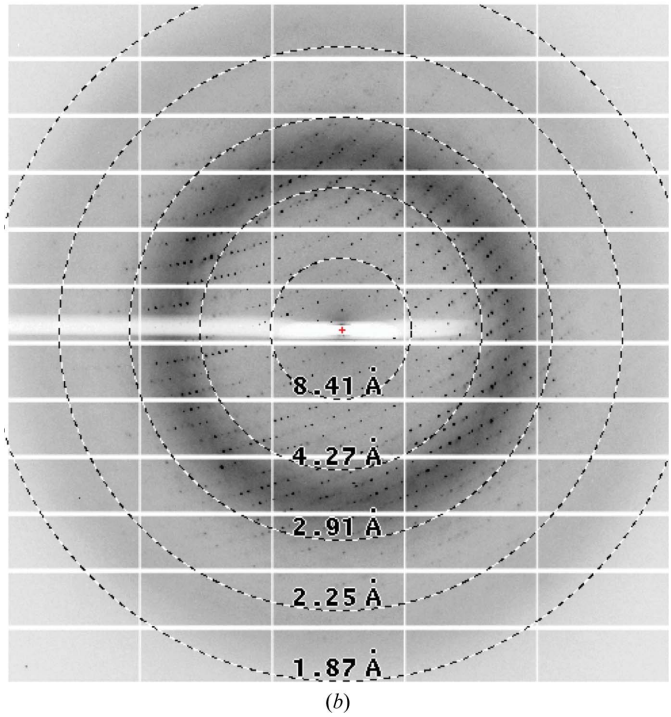

(*b*)

Figure 3
(*a*) Image of BabA$^{25–460}$–Nb-ER19 crystals and SDS–PAGE of dissolved crystals alongside purified BabA$^{25–460}$ (inset, labelled C and P, respectively; *, BabA$^{25–460}$; **, Nb-ER19). (*b*) Representative diffraction image (0.2° rotation, 0.2 s exposure at 20% transmission) from a crystal of BabA$^{25–460}$ in complex with Nb-ER19 obtained by the sitting-drop vapour-diffusion method.

We acknowledge the use of the synchrotron-radiation facility at Diamond Light Source, Didcot, England under proposal MX9426, and thank the staff of the Diamond MX group and beamline I04 for assistance during data collection. This work is supported by project grant PRJ9 from the Flanders Institute of Biotechnology (VIB), the Odysseus program of the Flanders Science Foundation (FWO) and equipment grant UABR/09/005 from the Hercules Foundation. SS is the recipient of an Erasmus Mundus PhD fellowship. TB is supported by grants from Vetenskapsrådet/VR and Cancerfonden.

References

Alm, R. A., Bina, J., Andrews, B. M., Doig, P., Hancock, R. E. W. & Trust, T. J. (2000). *Infect. Immun.* **68**, 4155–4168.
Aspholm-Hurtig, M. *et al.* (2004). *Science*, **305**, 519–522.
Backert, S. & Clyne, M. (2011). *Helicobacter*, **16**, 19–25.
Baranova, E., Fronzes, R., Garcia-Pino, A., Van Gerven, N., Papapostolou, D., Péhau-Arnaudet, G., Pardon, E., Steyaert, J., Howorka, S. & Remaut, H. (2013). *Nature (London)*, **487**, 119–122.

Borén, T., Falk, P., Roth, K. A., Larson, G. & Normark, S. (1993). *Science*, **262**, 1892–1895.
Delahay, R. M. & Rugge, M. (2012). *Helicobacter*, **17**, 9–15.
Every, A. L. (2013). *Trends Microbiol.* **21**, 253–259.
Gerhard, M., Lehn, N., Neumayer, N., Borén, T., Rad, R., Schepp, W., Miehlke, S., Classen, M. & Prinz, C. (1999). *Proc. Natl Acad. Sci. USA*, **96**, 12778–12783.
Ilver, D., Arnqvist, A., Ogren, J., Frick, I. M., Kersulyte, D., Incecik, E. T., Berg, D. E., Covacci, A., Engstrand, L. & Borén, T. (1998). *Science*, **279**, 373–377.
Kabsch, W. (2010). *Acta Cryst.* D**66**, 125–132.
Lo, A. W. H., Moonens, K. & Remaut, H. (2013). *Curr. Opin. Microbiol.* **16**, 85–92.
Matthews, B. W. (1968). *J. Mol. Biol.* **33**, 491–497.
Moore, M. E., Borén, T. & Solnick, J. V. (2011). *Gut Microbes*, **2**, 42–46.
Pang, S. S., Nguyen, S. T. S., Perry, A. J., Day, C. J., Panjikar, S., Tiralongo, J., Whisstock, J. C. & Kwok, T. (2014). *J. Biol. Chem.* **289**, 6332–6340.
Pardon, E., Laeremans, T., Triest, S., Rasmussen, S. G. F., Wohlkönig, A., Ruf, A., Muyldermans, S., Hol, W. G. J., Kobilka, B. K. & Steyaert, J. (2014). *Nature Protoc.* **9**, 674–693.
Steyaert, J. & Kobilka, B. K. (2011). *Curr. Opin. Struct. Biol.* **21**, 567–572.
Tomb, J. F. *et al.* (1997). *Nature (London)*, **388**, 539–547.